# ABSOLUTE CROSS SECTIONS OF TWO-NUCLEON TRANSFER REACTIONS INDUCED BY HEAVY IONS

E. MAGLIONE

*Dipartimento di Fisica Galileo Galilei, Università di Padova, I-35100 Padua, Italy and INFN, Legnaro, Italy*

G. POLLAROLO

*Istituto di Fisica Teorica dell'Università di Torino, I-10125 Turin, Italy and INFN, Sezióne di Torino, I-10125, Turin, Italy*

A. VITTURI

*Dipartimento di Fisica Galileo Galilei, Università di Padova, I-35100 Padua, Italy and INFN, Sezione di Padova, I-35100 Padua, Italy*

R.A BROGLIA and A. WINTHER

*The Niels Bohr Institute, University of Copenhagen, DK-2100 Copenhagen Ø, Denmark*

Received 2 April 1985; revised manuscript received 20 August 1985

Two-nucleon transfer reactions are calculated for a variety of reactions induced by $^{14}C$ and $^{16}O$. The contributions due to the successive and the simultaneous transfer of nucleons and the correction connected with the non-orthogonality of the basis states are included in the calculations. They reproduce the experimental cross sections within a factor of 3. The successive transfer of nucleons alone accounts for the major fraction of the predicted cross section.

The analysis of two-nucleon transfer reactions induced by heavy ions may allow to gain a better understanding of the role played by pairing correlations in nuclei. An important step in this program is the study of the different processes contributing to the associated absolute cross sections.

In what follows we present the analysis of the reactions [1] [‡1] $^{138}$Ba($^{14}$C, $^{12}$C)$^{140}$Ba(gs), $^{124}$Sn($^{14}$C, $^{12}$C)$^{126}$Sn(gs) and $^{208}$Pb($^{16}$O, $^{18}$O)$^{206}$Pb(gs) at energies both above and below the Coulomb barrier. The cross section

$$d\sigma(\theta)/d\Omega = |f(\theta)|^2 , \tag{1}$$

is calculated making use of the partial wave expansion

$$f(\theta) = \frac{1}{2k} \sum_l (2l+1) \exp[2i(\sigma_l + \delta_l)] a(l) P_l(\cos\theta) , \tag{2}$$

where $\sigma_l$ and $\delta_l$ are the Coulomb and nuclear phase shifts.

The transfer amplitude

‡1 See also ref. [2] as quoted in ref. [3].

$$a(l) = [a(l)]_{(1)} + [a(l)]_{\mathrm{succ}} + [a(l)]_{\mathrm{orth}} \tag{3}$$

is the sum of the contributions associated with the simultaneous and the successive transfer of nucleons. The last term contains the non-orthogonality correction [4–7]. These amplitudes are expressed in terms of the single-particle formfactors and overlaps $f$ and $g$ defined in refs. [8,9]. For the case of two-nucleon transfer processes between even nuclei connecting the ground or $0^+$ excited states in both target and projectile one can write

$$[a(l)]_{(1)} = -\mathrm{i} \sum_{a_1 a_1'} B^{(\mathrm{A})}(a_1 a_1; 0)\, B^{(\mathrm{b})}(a_1' a_1'; 0) \left(\frac{2j_1' + 1}{2j_1 + 1}\right)^{1/2} \sum_{\lambda\mu'} \frac{(-1)^{\lambda+\mu'}}{2\lambda+1}$$

$$\times\, 2 \int_{-\infty}^{\infty} \frac{\mathrm{d}t}{\hbar}\, \tilde{f}^{a_1 a_1'}_{\lambda\mu'}(k_\| k_\perp r)\, \tilde{g}^{a_1 a_1'}_{\lambda-\mu'}(k_\| k_\perp r) \exp\{(\mathrm{i}/\hbar)[(E_\beta - E_\alpha)t + \gamma_{\beta\alpha}(t)]\}\,, \tag{4}$$

$$[a(l)]_{\mathrm{orth}} = \mathrm{i} \sum_{\substack{a_1 a_1' \\ I_\mathrm{F} I_\mathrm{f}}} B^{(\mathrm{A})}(a_1 a_1; 0)\, B^{(\mathrm{b})}(a_1' a_1'; 0) |C^{(\mathrm{A})}(0a_1; I_\mathrm{F})|^2 |C^{(\mathrm{b})}(0a_1'; I_\mathrm{f})|^2 \left(\frac{2j_1' + 1}{2j_1 + 1}\right)^{1/2}$$

$$\times \sum_{\lambda\mu'} \frac{(-1)^{\lambda+\mu'}}{2\lambda+1}\, 2 \int_{-\infty}^{\infty} \frac{\mathrm{d}t}{\hbar}\, \tilde{f}^{a_1 a_1'}_{\lambda\mu'}(k_\| k_\perp r)\, \tilde{g}^{a_1 a_1'}_{\lambda-\mu'}(k_\| k_\perp r) \exp\{(\mathrm{i}/\hbar)[(E_\beta - E_\alpha)t + \gamma_{\beta\alpha}(t)]\}\,, \tag{5}$$

and

$$[a(l)]_{\mathrm{succ}} = -\sum_{\substack{a_1 a_1' \\ \gamma I_\mathrm{f} I_\mathrm{F}}} B^{(\mathrm{A})}(a_1 a_1; 0) B^{(\mathrm{b})}(a_1' a_1'; 0) |C^{(\mathrm{A})}(0a_1; I_\mathrm{F})|^2 |C^{(\mathrm{b})}(0a_1'; I_\mathrm{f})|^2 \left(\frac{2j_1' + 1}{2j_1 + 1}\right)^{1/2}$$

$$\times \sum_{\lambda\mu\mu'\mu''} \frac{(-1)^{\lambda+\mu}}{2\lambda+1} D^{\lambda}_{\mu\mu'}(0\,\tfrac{1}{2}\pi\,0)\, D^{\lambda}_{-\mu\mu''}(0\,\tfrac{1}{2}\pi\,0)$$

$$\times \int_{-\infty}^{\infty} \frac{\mathrm{d}t}{\hbar}\, \tilde{f}^{a_1 a_1'}_{\lambda\mu'}(k_\| k_\perp r) \exp\{(\mathrm{i}/\hbar)[(E_\beta - E_\gamma)t + \gamma_{\beta\gamma}(t) + \mathrm{i}\mu\phi(t)]\}$$

$$\times \int_{-\infty}^{t} \frac{\mathrm{d}t'}{\hbar}\, \tilde{f}^{a_1 a_1'}_{\lambda\mu''}(k_\| k_\perp r) \exp\{(\mathrm{i}/\hbar)[(E_\gamma - E_\alpha)t' + \gamma_{\gamma\alpha}(t') - \mathrm{i}\mu\phi(t')]\}\,. \tag{6}$$

The indices $\alpha$, $\gamma$ and $\beta$ label the initial [$\alpha$ = a(b + 2) + A], intermediate [$\gamma$ = f(= b + 1) + F] and final [$\beta$ = b + B(= A + 2)] channels. The quantum numbers $a_1 = (n_1, l_1, j_1)$ and $a_1' = (n_1', l_1', j_1')$ label the single-particle levels in target and projectile respectively.

The formfactors $f$ and overlaps $g$ in the intrinsic frame are defined in eq. (6.10) of ref. [9]. They depend on the distance $r(t)$ between the ions and on the longitudinal and transverse components $k_\|(t)$ and $k_\perp(t)$ of the wavenumber of relative motion associated with the transferred particle. We use the approximation of including the longitudinal recoil effect, only through an average phase. We thus are

$$\tilde{f}^{a_1 a_1'}_{\lambda\mu}(k_\| k_\perp r) = \exp[\mathrm{i}\bar{\sigma}^{(\alpha)}]\, \tilde{f}^{a_1 a_1'}_{\lambda\mu}(0 k_\perp r)\,, \quad \tilde{g}^{a_1 a_1'}_{\lambda\mu}(k_\| k_\perp r) = \exp[\mathrm{i}\bar{\sigma}^{(\alpha)}]\, \tilde{g}^{a_1 a_1'}_{\lambda\mu}(0 k_\perp r)\,,$$

where

$$\bar{\sigma} = k_\| \{z_{\max} - [m_\mathrm{A}/(m_\mathrm{a} + m_\mathrm{A})] r\}\,,$$

$z_{\max}$ being the distance from the target where the integrand in the formfactor is maximum. The integrals are carried out over a trajectory obtained by averaging the entrance and exit channel trajectories. Because the formfactors are short ranged, one can approximate the trajectory with the expression [8]

$$r(t) = r_0 + \tfrac{1}{2}\ddot{r}_0 t^2 , \quad \phi(t) = \dot{\phi}_0 t . \tag{7a}$$

Here $r_0$ is the complex classical turning point, and $\dot{\phi}_0$ and $\ddot{r}_0$ are the angular velocity and radial acceleration at this point.

Correspondingly we expand the phase $\gamma(t)$ and $\bar{\sigma}(t)$ through

$$\gamma(t) = \dot{\gamma} t , \quad \bar{\sigma}(t) = \dot{\bar{\sigma}} t , \quad k_\perp = (l/r_0)(m_a + m_A)/m_a m_A . \tag{7b}$$

The quantity $\dot{\gamma}$ is given by

$$\dot{\gamma}_{\beta\alpha} = [(m_A - m_b)/(m_a + m_A)] v^2(0) + U_{bB}(r_0) - U_{aA}(r_0) , \tag{8}$$

and correspondingly for $\dot{\gamma}_{\beta\gamma}$ and $\dot{\gamma}_{\gamma\alpha}$. The quantity $v(0)$ is the velocity at the turning point. The average recoil phases are in the prior representation

$$\dot{\bar{\sigma}}^{(\alpha)}_{\gamma\alpha} \approx \dot{\bar{\sigma}}^{(\alpha)}_{\beta\gamma} = (M/\hbar)\, \ddot{r}_0 \{R_A - [m_A/(m_a + m_A)] r\} , \tag{9a}$$

while

$$\dot{\bar{\sigma}}^{(\sigma)}_{\gamma\alpha} = (M/\hbar)\, \ddot{r}_0 \{\tfrac{1}{2} r + 0.725(R_A - R_a) - [m_A/(m_a + m_A)] r\} , \tag{9b}$$

where $M$ is the nucleon mass, and where we used $R_A = 1.0 A^{1/3}$ fm.

The quantities $|C|^2$ are the one-nucleon spectroscopic factors, while the $B$ denote the two-nucleon spectroscopic amplitudes. For the case to be analyzed below we use $|C|^2 = 1$ for the intermediate single-particle states. We use furthermore

$$B^{(A)}(a_1 a_1; 0) = (-1)^{l_1} \sqrt{j_1 + 1/2}\, U_{a_1} V_{a_1} , \tag{10a}$$

$$= (-1)^{l_1} X_{a_1} , \tag{10b}$$

and

$$B^{(b)}(a_1' a_1'; 0) = (-1)^{l} X_{a_1'} . \tag{11}$$

The quantity $V^2_{a_1} = 1 - U^2_{a_1}$ is the occupation probability of the orbital $a_1$ in the case of a superfluid nucleus, while $X_{a_1}$ is the amplitude of a two-hole state in the closed shell system B. Similarly $X_{a_1}$ is the amplitude of a two-particle state moving around the core b. Both $X_{a_1}$ and $X_{a_1'}$ are calculated in the Tamm–Dancoff approximation. On the other hand (static) ground state correlations are included in the spectroscopic factor (10a) associated with the superfluid system.

Making use of the correlated wavefunctions and $U$, $V$ coefficients shown in tables 1, 2 the two-nucleon spectroscopic amplitudes were obtained.

In the calculation of the single-particle wavefunctions entering in formfactors and overlaps two different prescriptions have been used. For those associated with the simultaneous amplitude, each of the particles were bound by one-half of the two-nucleon separation energy, while the experimental energies were used in calculating (5) and (6).

Only the terms with $\mu' = 0$ and maximum value of $\lambda$ for each pair of configurations were taken into account in eqs. (4)–(6). Contributions to (4) arising from $\mu' \neq 0$, were found to amount to less than 10% of the $\mu' = 0$ amplitude.

Cross sections arising from the simultaneous transfer amplitude (4) are compared in table 3 with the corresponding cross section associated with a quantal description of the process and calculated making use of the codes TWOFF and DIWRI [3]. The quantal results are typically 50% smaller than the semiclassical estimates.

The calculations were further tested by comparing our predicted semiclassical successive differential cross sections associated with the reaction $^{208}$Pb($^{16}$O, $^{18}$O)$^{206}$Pb at an energy below that of the Coulomb barrier, with

Table 1
Amplitudes defining the wave functions of the different nuclei in the reactions considered and used to construct the two-particle transfer spectroscopic amplitudes (10) and (11). For $^{206}$Pb(gs) and $^{140}$Ba(gs) they are the results of a pairing calculation for two neutron holes in the $N$ = 126 core, and two neutron particles outside the $N$ = 82 core, respectively. Experimental energies for the single-particle orbitals have been used. The pairing strength was fixed to reproduce the experimental binding energies of $^{206}$Pb and $^{140}$Ba. For $^{18}$O and $^{14}$C, described as two-neutrons outside the $^{16}$O and $^{12}$C cores respectively empirical wave functions were used (cf. refs. [4,10]).

| Nuclei | $n, l, j$ | $X$ |
|---|---|---|
| $^{206}$Pb(gs) | $2p_{1/2}$ | 0.75 |
| | $1f_{5/2}$ | 0.47 |
| | $2p_{3/2}$ | 0.28 |
| | $0i_{13/2}$ | −0.28 |
| | $1f_{7/2}$ | 0.18 |
| | $0h_{9/2}$ | 0.14 |
| $^{140}$Ba(gs) | $1f_{7/2}$ | 0.77 |
| | $2p_{3/2}$ | 0.31 |
| | $2p_{1/2}$ | 0.17 |
| | $0h_{9/2}$ | 0.34 |
| | $1f_{5/2}$ | 0.24 |
| | $0i_{13/2}$ | −0.35 |
| $^{18}$O(gs) | $0d_{5/2}$ | 0.89 |
| | $1s_{1/2}$ | 0.45 |
| $^{14}$C(gs) | $0p_{1/2}$ | 0.95 |
| | $0d_{5/2}$ | −0.29 |
| | $1s_{1/2}$ | −0.11 |

Table 2
$U$, $V$ factors defining the wave functions of $^{124}$Sn and $^{126}$Sn in the reactions considered and used to construct the two-particle transfer spectroscopic amplitudes (10). The pairing coupling constant was chosen to reproduce in both nuclei a pairing gap $\Delta \approx 1.2$ MeV.

| $n, l, j$ | $U$ (A) | |
|---|---|---|
| | $^{124}$Sn | $^{126}$Sn |
| $1p_{3/2}$ | 0.07 | 0.07 |
| $0f_{5/2}$ | 0.07 | 0.07 |
| $1p_{1/2}$ | 0.08 | 0.08 |
| $0g_{9/2}$ | 0.10 | 0.10 |
| $1d_{5/2}$ | 0.18 | 0.17 |
| $0g_{7/2}$ | 0.21 | 0.20 |
| $2s_{1/2}$ | 0.32 | 0.28 |
| $1d_{3/2}$ | 0.40 | 0.35 |
| $0h_{11/2}$ | 0.79 | 0.71 |
| $1f_{7/2}$ | 0.98 | 0.97 |
| $0h_{9/2}$ | 0.99 | 0.98 |
| $0i_{13/2}$ | 0.99 | 0.99 |
| $2p_{3/2}$ | 0.99 | 0.99 |
| $1f_{5/2}$ | 0.99 | 0.99 |
| $2p_{1/2}$ | 0.99 | 0.99 |

the quantal results of ref. [7] and the semiclassical results of ref. [6]. The agreement between the two calculations was satisfactory.

Optical potentials empirically determined [1,2] from the fitting of elastic scattering cross sections were used in calculating the semiclassical differential cross sections shown in fig. 1.

While the calculated differential cross sections associated with the reactions $^{124}$Sn($^{14}$C, $^{12}$C)$^{126}$Sn(gs) and $^{208}$Pb($^{16}$O, $^{18}$O)$^{206}$Pb(gs) are in satisfactory agreement with the data, the one associated with the reaction $^{138}$Ba($^{14}$C,$^{12}$C)$^{140}$Ba(gs) is a factor 6 larger. This discrepancy, which is expected to persist also in a quantal calculation (cf. table 3), is not understood at present.

As was to be expected the relative importance of the simultaneous contribution and non-orthogonality correction is connected with the pairing collectivity displayed by wavefunctions describing the motion of the transferred nucleons. Thus, in the case of the reactions $^{208}$Pb($^{16}$O, $^{18}$O)$^{206}$Pb(gs) and $^{124}$Sn($^{14}$C, $^{12}$C)$^{126}$Sn(gs) the simultaneous transfer cross section is a factor of 7 and 2.4 smaller than the successive transfer, respectively. The situation encountered in the case of the reaction $^{138}$Ba($^{14}$C, $^{12}$C)$^{140}$B(gs) is intermediate. In all cases the non-orthogonality contribution has a strong tendency to cancel the simultaneous (first-order) contribution, as it would exactly do for the transfer of independent particles.

Table 3
Ratio $R = \sigma_{quantal}/\sigma_{semiclassical}$ of the cross section arising from the simultaneous transfer amplitude (4) and the corresponding quantal results at energies above and below the Coulomb barrier $E_B$. The latter have been calculated with the computer codes TWOFF and DIWRI [3], with the prescription of scaling the coordinate in the distorted waves in correspondence with the recoil phase (9) (cf. ref. [9]). For each reaction the pure configurations shown in the first column have been used.

| Reaction | $E < E_B$ | | $E > E_B$ | |
|---|---|---|---|---|
| | $E$ (MeV) | $R$ | $E$ (MeV) | $R$ |
| $^{208}Pb(^{16}O, ^{18}O(0d_{5/2}))^{206}Pb(2p_{1/2})$ | 70 | 0.5 | 86 | 0.4 |
| $^{124}Sn(^{14}C, ^{12}C(0p_{1/2}))^{126}Sn(1f_{7/2})$ | 38 | 0.7 | 59.7 | 0.5 |
| $^{138}Ba(^{14}C, ^{12}C(0p_{1/2}))^{140}Ba(1f_{7/2})$ | 45 | 0.6 | 64 | 0.4 |

A measure of the sensitivity of two-nucleon transfer reactions to pairing correlations is provided by the enhancement of the calculated cross sections with respect to pure configurations (cf. table 4). Thus, the largest enhancement is found for the simultaneous transfer of a pair in the case $^{124}Sn(^{14}C, ^{12}C)^{126}Sn$ reaction. The successive transfer of particles display the same type of constructive coherence as the simultaneous transfer and lead to enhancement factors which are similar to those displayed by the simultaneous transfer contribution.

In table 4 we have also collected the enhancement factors associated with the $^{208}Pb(p,t)^{206}Pb(gs)$, $^{138}Ba(t,p)^{140}Ba(gs)$, and $^{124}Sn(t,p)^{126}Sn(gs)$ cross sections, which are calculated only for the simultaneous transfer of particles. The resulting enhancement factors are very similar to those associated with the heavy ion transfer processes.

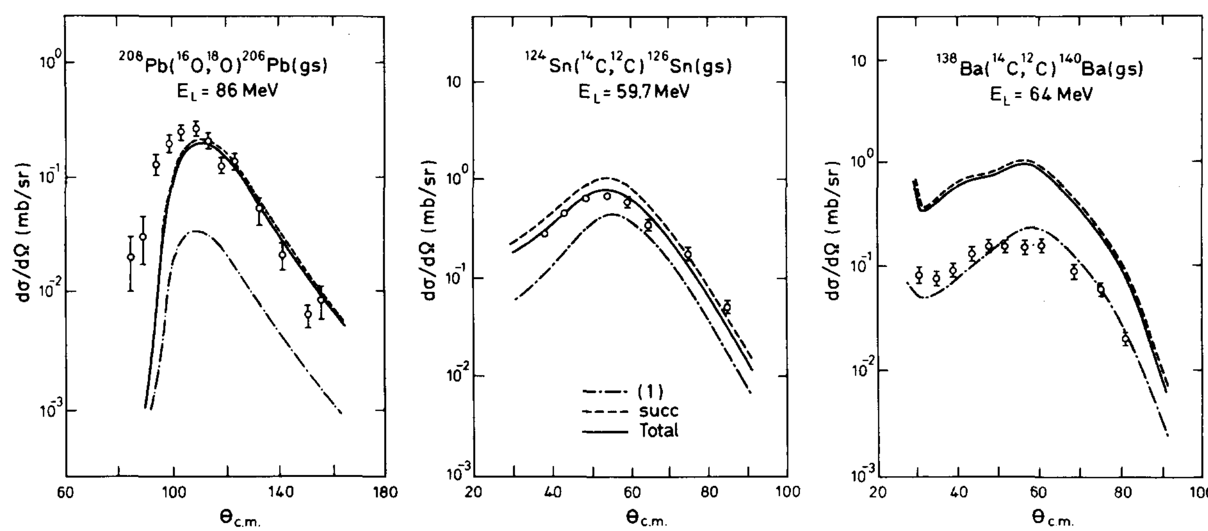


Fig. 1. Calculated angular distributions for two-particle transfer reactions compared with experimental data (refs. [1,2]). Also shown are the cross sections obtained by only including the one-step simultaneous transfer and the two-step successive transfer, while the solid lines gives the results obtained when both contributions are taken into account, together with the non-orthogonality term.

Table 4
Cross sections for pure two-particle configurations in the target compared with those obtained using the correlated wave functions. For the projectiles the wave functions of tables 1, 2 have been used in all cases. The numbers in the last row for each reaction give the enhancement factors $\epsilon$ defined in terms on the averaged pure two-particle cross sections. The cross sections for (t, p) reactions have been calculated microscopically making use of the computer code DWUCK [11].

| Reaction | $\theta$ (°) | $n,l,j$ | $d\sigma(\theta)/d\Omega$ | | | |
|---|---|---|---|---|---|---|
| | | | | 1-step | 2-step | Total |
| $^{206}Pb(t, p)^{208}Pb$ | 0 | $2p_{1/2}$ | 31.5 | | | |
| | | $1f_{5/2}$ | 16.7 | | | |
| | | $2p_{3/2}$ | 70.4 | | | |
| | | $0i_{13/2}$ | 1.1 | | | |
| | | $1f_{7/2}$ | 34.1 | | | |
| | | $0h_{9/2}$ | 0.7 | | | |
| | | total | 100.0 | | | |
| | | $\epsilon$ | 3.9 | | | |
| $^{208}Pb(^{16}O, ^{18}O)^{206}Pb(gs)$ | 112 | $2p_{1/2}$ | | 11.5 | 98.3 | 95.0 |
| | | $1f_{5/2}$ | | 9.6 | 72.1 | 68.0 |
| | | $2p_{3/2}$ | | 13.0 | 63.8 | 57.0 |
| | | $0i_{13/2}$ | | 0.08 | 0.5 | 0.5 |
| | | $1f_{7/2}$ | | 4.0 | 12.2 | 9.2 |
| | | $0h_{9/2}$ | | 1.2 | 6.5 | 5.4 |
| | | total | | 31.5 | 214.0 | 200.0 |
| | | $\epsilon$ | | 4.8 | 5.1 | 5.1 |
| $^{126}Sn(p, t)^{124}Sn(gs)$ | 0 | $2s_{1/2}$ | 15.6 | | | |
| | | $1d_{3/2}$ | 7.0 | | | |
| | | $0h_{11/2}$ | 0.6 | | | |
| | | $0f_{7/2}$ | 12.9 | | | |
| | | $0h_{9/2}$ | 0.1 | | | |
| | | total | 100.0 | | | |
| | | $\epsilon$ | 14.0 | | | |
| $^{124}Sn(^{14}C, ^{12}C)^{126}Sn(gs)$ | 56 | $2s_{1/2}$ | | 49.8 | 189.0 | 161.0 |
| | | $1d_{3/2}$ | | 16.3 | 73.0 | 64.0 |
| | | $0h_{11/2}$ | | 4.4 | 14.3 | 14.0 |
| | | $1f_{7/2}$ | | 68.7 | 207.0 | 167.0 |
| | | $0h_{9/2}$ | | 0.9 | 5.0 | 4.1 |
| | | total | | 441.0 | 1050.0 | 785.0 |
| | | $\epsilon$ | | 15.7 | 10.7 | 9.6 |

*Continued on next page*

Table 4 (continued)

| Reaction | $\theta$ (°) | $n, l, j$ | $d\sigma(\theta)/d\Omega$ | | | |
|---|---|---|---|---|---|---|
| | | | | 1-step | 2-step | Total |
| $^{138}Ba(t, p)^{140}Ba(gs)$ | 0 | $1f_{7/2}$ | 32.4 | | | |
| | | $2p_{3/2}$ | 75.0 | | | |
| | | $2p_{1/2}$ | 37.5 | | | |
| | | $0h_{9/2}$ | 1.8 | | | |
| | | $1f_{5/2}$ | 24.5 | | | |
| | | $0i_{13/2}$ | 2.3 | | | |
| | | total | 100.0 | | | |
| | | $\epsilon$ | 3.45 | | | |
| $^{138}Ba(^{14}C, ^{12}C)^{140}Ba(gs)$ | 58 | $1f_{7/2}$ | | 128.0 | 553.0 | 511.0 |
| | | $2p_{3/2}$ | | 213.0 | 1136.0 | 1036.0 |
| | | $2p_{1/2}$ | | 50.0 | 300.0 | 266.0 |
| | | $0h_{9/2}$ | | 1.8 | 12.0 | 11.0 |
| | | $1f_{5/2}$ | | 23.0 | 121.0 | 106.0 |
| | | $0i_{13/2}$ | | 3.0 | 9.0 | 9.0 |
| | | total | | 273.0 | 1203.0 | 1115.0 |
| | | $\epsilon$ | | 3.9 | 3.4 | 3.45 |

Discussions with B. Bayman and B.S. Nilsson are gratefully acknowledged.

## *References*


[1] W. von Oertzen, R.E. Brown, E.R. Flynn, S.C. Peng and J.W. Sunier, Z. Phys. A313 (1983) 371.
[2] J.S. Lilley, unpublished data.
[3] B.S. Nilsson, Computer codes TWOFF and DIWRI, unpublished.
[4] U. Götz, M. Ichimura, R.A. Broglia and A. Winther, Phys. Rep. 15C (1975) 115.
[5] D.H. Feng, T. Tamura, T. Udagawa, J. Lynch and K.S. Low, Phys. Rev. C14 (1976) 1484;
D.H. Feng, T. Udagawa and T. Tamura, Nucl. Phys. A274 (1976) 262.
[6] M.A. Franey, B.F. Bayman, J.S. Lilley and W.R. Phillips, Phys. Rev. Lett. 41 (1978) 1837.
[7] B.F. Bayman and J. Chen, Phys. Rev. C26 (1982) 1509.
[8] R.A. Broglia, G. Pollarolo and A. Winther, Nucl. Phys. A361 (1981) 307.
[9] R.A. Broglia, R. Liotta, B.S. Nilsson and A. Winther, Phys. Rep. 29C (1977) 291.
[10] F.E. Cecil, J.R. Shepard, R.E. Anderson, R.J. Peterson and P. Kaczkowski, Nucl. Phys. A255 (1975) 243.
[11] P.D. Kunz, Computer code DWUCK, unpublished.